SORET AND DUFOUR EFFECTS ON HYDROMAGNETIC FLOW OF EYRING-POWELL FLUID OVER OSCILLATORY STRETCHING SURFACE WITH HEAT GENERATION/ABSORPTION AND CHEMICAL REACTION

by

Sami ULLAH KHAN [a*,**], ***Nasir ALI*** [a], ***and Zaheer ABBAS*** [b]

[a] Department of Mathematics and Statistics, International Islamic University, Islamabad, Pakistan
[b] Department of Mathematics, The Islamia University of Bahawalpur, Bahawalpur, Pakistan

Original scientific paper
https://doi.org/10.2298/TSCI150831018U

In this article, we have investigated thermal-diffusion and diffusion-thermo effects on unsteady flow of electrically conducting Eyring-Powell fluid over an oscillatory stretching sheet by using convective boundary conditions. A set of appropriate variables are used to reduce number of independent variables in governing equations. Series solution is computed using homotopy analysis method. The effects of various parameters of interest on the velocity filed, temperature profile, concentration profile, skin friction, local Nusselt number and local Sherwood number are illustrated graphically and discussed in detail.

Key words: *Eyring-Powell fluid, Dufour number, oscillatory stretching sheet, Soret number*

Introduction

Recently, interest in boundary-layer flow with heat/mass transfer in the presence of chemical reaction has attracted the attention of researchers because of its several significant applications. Such applications include, food processing, cooling towers, packed sphere bed, spinning of fibers and many more. Another important application of such phenomenon can be encountered in power energy. These numerous applications lead the researchers to devote their attention to analyze the effects of heat and mass transfer in viscous and viscoelastic fluids over stretching surfaces. Alharbi *et al*. [1] investigated the flow of second grade fluid in presence of heat and mass transfer over porous stretching sheet. Numerical using fourth order Runge-Kutta method combined with shooting technique. Hayat *et al*. [2] studied the effects of heat and mass transfer in presence of chemical reaction in viscoelastic fluid-flow over stretching surface. Veena *et al*. [3] presented analytic solution in terms of Kummer's function for viscoelastic fluid--flow to analyze heat transfer phenomenon. The effects of heat and mass transfer in steady flow of second grade fluid were discussed by Sanjayanand and Khan [4]. The existence of multiple solutions in heat and mass transfer of MHD slip flow of the viscoelastic fluid over a stretching sheet was discussed by Turkyilmazoglu [5]. Hamad *et al*. [6] investigated the radiation effects in steady flow of viscous fluid with heat and mass transfer. Takhar *et al*. [7] used finite difference scheme to discuss viscous fluid-flow with heat mass transfer over a stretching surface. The MHD free convective flow along with heat and mass transfer and chemical reaction over a stretching sheet was discussed by Afify [8].

* Corresponding author, e-mail: sk_iiu@yahoo.com

** Now at: Department of Mathematics, COMSATS Institute of Information Technology, Sahiwal, Pakistan

In many situations, simultaneous effects of heat and mass transfer effects are observed during motion of the fluids. In this case the heat flux is produced by both temperatures as well as concentration gradients.

The occurrence of diffusion flux due to temperature gradient results in thermal-diffusion which is called Soret effects. The opposite effects are known as Dufour effects which are produced because of chemical potential gradient due to energy flux. The effects are encountered in geosciences and chemical industries. Anghel *et al.* [9] included Dufour and Soret effects in flow of viscous fluid over a porous vertical surface. Sunder *et al*. [10] used Darcian porous medium to predict Soret and Dufour effects in heat and mass transfer flow of Newtonian fluid over a vertical surface. The mixed convection flow of viscous fluid subject to Soret and Dufour effects was carried out by Srinivasacharya and RamReddy [11]. Beg *et al*. [12] presented numerical investigation of flow of viscous fluid subject to Soret and Dufour effects. Cheng [13] presented numerical study of Power law fluid with variables heat and mass fluxes and Soret and Dufour effects. The numerical computations were carried out by cubic spline collocation method and results were found in good agreement with earlier results. Shateyi *et al.* [14] examined the Soret and Dufour effects along with hall currents and mixed convection on MHD flow over a vertical surface. The viscous fluid-flow in presence of Soret and Dufour effects over oscillatory stretching sheet was analyzed by Zheng *et al*. [15]. This work was recently extended by Ali *et al*. [16] for viscoelastic fluid flow in a porous medium.

The literature survey previously provided indicates that Soret and Dufour effects in presence of chemical reaction in unsteady laminar flow of Eyring-Powell fluid [16-22] over an oscillatory stretching sheet are still not investigated. The aim of present work is to carry out such an analysis. The heat transfer problem is formulated by using convective boundary conditions. Series solution is computed using homotopy analysis method [23-26]. Results obtained through computations are illustrated graphically for several values of parameters of interest.

Flow analysis

Consider time-dependent laminar boundary-layer flow of incompressible electrically conducting Eyring-Powell fluid over an oscillatory stretching sheet. The stretching sheet is oscillating with velocity $u = u_\omega = b\bar{x}\sin\omega_t$ where b denote the stretching rate and ω is the angular frequency. Let T_f and T_∞ denotes convective fluid temperature below the sheet and free stream temperature, respectively. Let C_w represents the concentration at the wall while the concentration far away from the surface is denoted by C_∞. A constant magnetic field of strength B_0 is imposed normal to sheet. A schematic diagram of the flow geometry is illustrated in fig. 1. The boundary-layer equations for flow under consideration are:

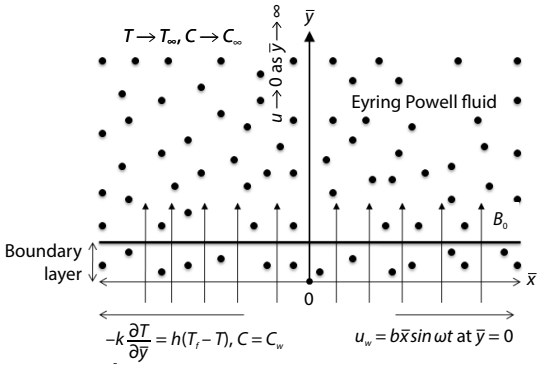

Figure 1. Geometry of the problem

$$\frac{\partial u}{\partial \bar{x}} + \frac{\partial v}{\partial \bar{y}} = 0 \tag{1}$$

$$\frac{\partial u}{\partial t}+u\frac{\partial u}{\partial \bar{x}}+v\frac{\partial v}{\partial \bar{y}}=\left(\nu+\frac{1}{\rho\beta c}\right)\frac{\partial^2 u}{\partial \bar{y}^2}-\frac{1}{2\rho\beta c^3}\left(\frac{\partial u}{\partial \bar{y}}\right)^2\frac{\partial^2 u}{\partial \bar{y}^2}-\frac{\sigma B_0^2 u}{\rho} \tag{2}$$

$$\frac{\partial T}{\partial t}+u\frac{\partial T}{\partial \bar{x}}+v\frac{\partial T}{\partial \bar{y}}=\alpha\frac{\partial^2 T}{\partial \bar{y}^2}+\frac{D_m k_T}{c_s c_p}\frac{\partial^2 C}{\partial \bar{y}^2}+\frac{Q}{\rho c_p}\left(T-T_\infty\right) \tag{3}$$

$$\frac{\partial C}{\partial t}+u\frac{\partial C}{\partial \bar{x}}+v\frac{\partial C}{\partial \bar{y}}=D_m\frac{\partial^2 C}{\partial \bar{y}^2}+\frac{D_m k_T}{T_m}\frac{\partial^2 T}{\partial \bar{y}^2}-k_1\left(C-C_\infty\right) \tag{4}$$

The eqs. (1)-(4) are subject to the following boundary conditions:

$$u=u_w=b\bar{x}\sin\omega t,\quad v=\pm v_w,\quad -k\frac{\partial T}{\partial \bar{y}}=h\left(T_f-T\right),\quad C=C_w,\quad \text{at}\quad \bar{y}=0,\ t>0 \tag{5}$$

$$u\to 0,\quad T\to T_\infty,\quad C\to C_\infty\quad \text{as}\quad \bar{y}=\infty \tag{6}$$

where the velocity component u and v are taken along $\bar{x}$- and $\bar{y}$-directions, respectively, ν represents the kinematic viscosity, ρ – the density, β and c – the parameters of Eyring-Powell model, σ – the electrical conductivity, v_w – the suction ($v_w < 0$) or injection ($v_w > 0$) parameter, c_p – the specific heat, T – the temperature, α – the thermal diffusivity, k_T – the thermal diffusion ratio, D_m – the molecular diffusivity, T_m – the mean fluid temperature, c_s – the concentration susceptibility, h – the heat transfer coefficient, Q – the volumetric heat transfer, k_1 – the reaction rate constant. In eq. (5) the last expression represents the convective boundary conditions, in which h denotes the heat transfer coefficient and k is the thermal conductivity of the fluid. The appropriate dimensionless variables are [15]:

$$y=\sqrt{\frac{b}{\nu}}\bar{y},\qquad \tau=t\omega,\qquad u=b\bar{x}f_y\left(y,\tau\right),\quad v=-\sqrt{\nu b}f\left(y,\tau\right) \tag{7}$$

$$\theta(y,\tau)=\frac{T-T_\infty}{T_f-T_\infty},\qquad \phi(y,\tau)=\frac{C-C_\infty}{C_w-C_\infty} \tag{8}$$

Making previous variables, eq. (1) is satisfied identically and eqs. (2)-(4) transform to:

$$\left(1+K\right)f_{yyy}-Sf_{y\tau}-f_y^2+ff_{yy}\mathrm{Ha}^2 f_y-K\lambda f_{yy}^2 f_{yyy}=0 \tag{9}$$

$$\theta_{yy}+\mathrm{Pr}\left(\mathrm{Du}\phi_{yy}+f\theta_y-S\theta_\tau\right)+\mathrm{Pr}\,\gamma\theta=0 \tag{10}$$

$$\phi_{yy}+\mathrm{Sc}\left(\mathrm{Sr}\theta_{yy}+f\phi_y-S\theta_\tau\right)-\beta\mathrm{Sc}\phi=0 \tag{11}$$

The boundary conditions govern in eqs. (5) and (6) become:

$$f_y\left(0,\tau\right)=\sin\tau,\quad f\left(0,\tau\right)=f_w,\quad \theta_y(0,\tau)=-\gamma_1\left[1-\theta\left(0,\tau\right)\right],\quad \phi\left(0,\tau\right)=1 \tag{12}$$

$$f_y\left(\infty,\tau\right)=0,\quad \theta(\infty,\tau)=0,\quad \phi(\infty,\tau)=0 \tag{13}$$

In previous equations $K = 1/\mu\beta C$ and $\lambda = \bar{x}^2 b^3/2\nu C^2$ are the dimensionless Eyring-Powell fluid parameters. The parameter λ is the local non-Newtonian parameter because of its dependence on the length scale $\bar{x}$. Due to this dependence λ varies along the flow direction and thus the solution of eq. (9) is locally similar [18]. The graphical results for particular value of λ represent the variation in flow along the vertical direction at a specific longitudinal position $\bar{x}$. Moreover, $S \equiv \omega/b$ denotes the ratio of oscillation frequency to stretching rate, $\mathrm{Ha}^2 = \sigma B_0^2/\rho b$ – the Hartmann number, $f_w = -v_w/(b\nu)^{1/2}$ – suction ($f_w > 0$) or wall injection ($f_w < 0$) pa-

rameter, Pr = ν/α – the Prandtl number, Du = $D_m k_T (C_w - C_\infty) / c_s c_p \nu (T_f - T_\infty)$ – the Dufour number, Sr = $D_m k_T (T_f - T_\infty) / T_m \nu (C_w - C_\infty)$ – the Soret number, Sc = ν / D_m – the Schmidt number, $\beta = k_1 / b$ – the chemical reaction parameter, $\gamma = Q / b\rho c_p$ – the heat generation ($\gamma > 0$) or absorption ($\gamma < 0$) parameter, and $\gamma_1 = (h/k)(\nu/b)^{1/2}$ – the Biot number.

The mathematical expression for the skin-friction coefficient, Nusselt number and and Sherwood number can be expressed:

$$C_f = \frac{\tau_w}{\rho u_w^2}, \quad \mathrm{Nu} = \frac{\bar{x} q_w}{k\left(T_f - T_\infty\right)}, \quad \mathrm{Sh} = \frac{\bar{x} q_m}{D_B\left(C_w - C_\infty\right)} \tag{14}$$

where shear stress, surface heat flux, and mass flux are denoted by τ_w, q_w, and q_m, respectively. Using eqs. (7) and (8), eq. (14) takes the following form:

$$\sqrt{\mathrm{Re}_x} C_f = \left[\left(1+K\right) f_{yy} - \frac{K}{3}\lambda f_{yy}^3\right]_{y=0}, \quad \mathrm{Nu}\sqrt{\frac{1}{\mathrm{Re}_x}} = -\theta_y\left(0,\tau\right), \quad \sqrt{\frac{1}{\mathrm{Re}_x}}\mathrm{Sh} = -\phi_y\left(0,\tau\right) \tag{15}$$

where $\mathrm{Re}_x = u_w \bar{x} / \nu$ is the local Reynolds number.

Homotopy analysis method

To compute series solution of eqs. (9)-(11) with boundary conditions of eqs. (12) and (13), we use homotopy analysis method. To start our simulation, the approximate initial guesses are:

$$f_0(y,\tau) = f_w + \sin\tau\left[1 - \exp(-y)\right], \quad \theta_0(y) = \frac{\gamma}{\gamma+1}\exp(-y), \phi_0(y) = \exp(-y) \tag{16}$$

We define linear operators:

$$\pounds_f(f) = \frac{\partial^3 f}{\partial y^3} - \frac{\partial f}{\partial y}, \quad \pounds_\theta(f) = \frac{\partial^2 f}{\partial y^2} - f, \quad \pounds_\phi(f) = \frac{\partial^2 f}{\partial y^2} - f \tag{17}$$

satisfying:

$$\pounds_f[A_1 + A_2\exp(y) + A_3\exp(-y)] = 0 \tag{18}$$

$$\pounds_\theta[A_4\exp(y) + A_5\exp(-y)] = 0 \tag{19}$$

$$\pounds_\theta[A_6\exp(y) + A_7\exp(-y)] = 0 \tag{20}$$

where A_i (i = 1, 2,..., 7) appeared in eqs. (16)-(18) are constants.

The further procedural details of this method can be found in [23] and the latest book by Liao [26].

Result and discussion

It is well established fact that the auxiliary parameters play an important role within the frame of the homotopy analysis method. The rate of convergence depends upon the proper choice of these parameters. To highlight convergence region, we draw the h-curves in figs. 2(a)-2(c). We see that these curves predict that convergent solution for temperature, velocity and concentration fields can be obtained when $-1.1 \le h_f \le -0.1$, $-1.5 \le h_\theta \le 0.5$, and $-1.3 \le h_\phi \le -0.4$.

Figures 3(a) and 3(b) displays the variation of velocity with time under influence of two important parameters namely, Eyring fluid parameter, K, and Hartmann number. From fig. 3(a), we observe that velocity shows oscillatory behavior and its amplitude increases with increasing K. Figure 3(b) elucidates the effects of suction/blowing parameter, f_w, on dimensionless velocity profile f'. It is noticed that a phase shift occurs and amplitude of velocity decreases with increasing suction/blowing parameter f_w.

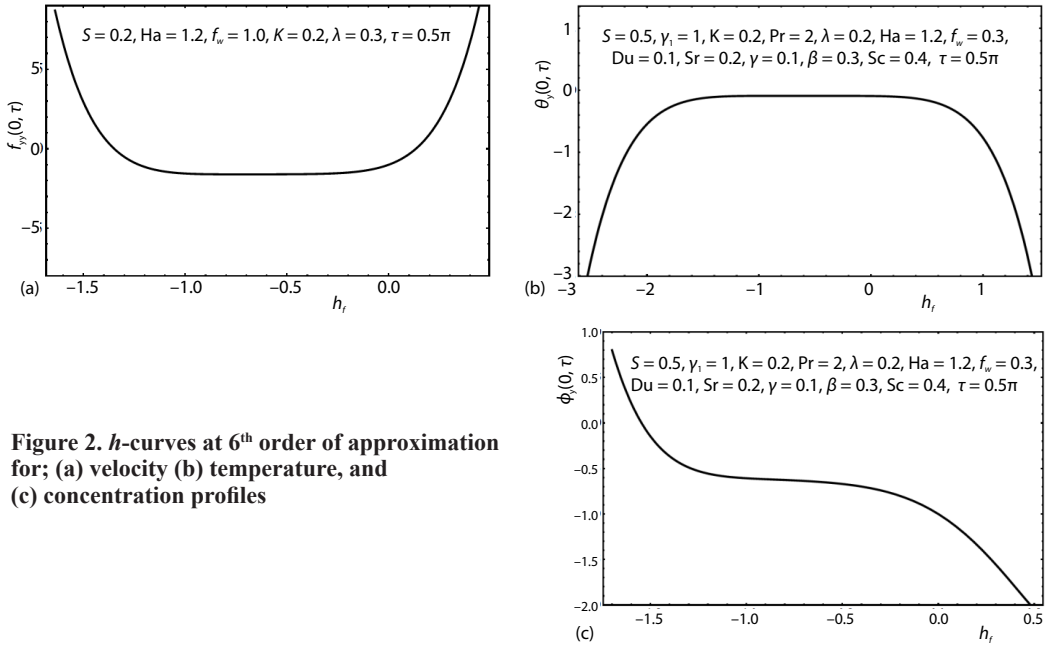

Figure 2. *h*-curves at 6th order of approximation for; (a) velocity (b) temperature, and (c) concentration profiles

The effects of Eyring-Powell fluid parameter, Hartmann number, and suction/injection parameter on transverse distribution of velocity at a time $\tau = \pi/2$ are shown in fig. 4. Figure 4(a) depicts that velocity increase with increasing the Eyring-Powell fluid parameter. Figure 4(b) depicts that the velocity profile decreases rapidly with increasing the Hartmann number, Moreover, the boundary-layer thickness also decreases in this case. From fig. 4(c), it has been noticed that increase in suction/blowing parameter, f_w, causes the thinning of the boundary-layer and velocity profile decreases with increasing suction/blowing parameter.

The influence of K on both temperature and concentration profiles at $\tau = \pi/2$ is shown in fig. 5. A significant decreasing effect in temperature is seen near the wall. Similar effects are observed in fig. 5(b). However, the change in concentration field with increasing K is smaller as compared to the corresponding change in temperature field.

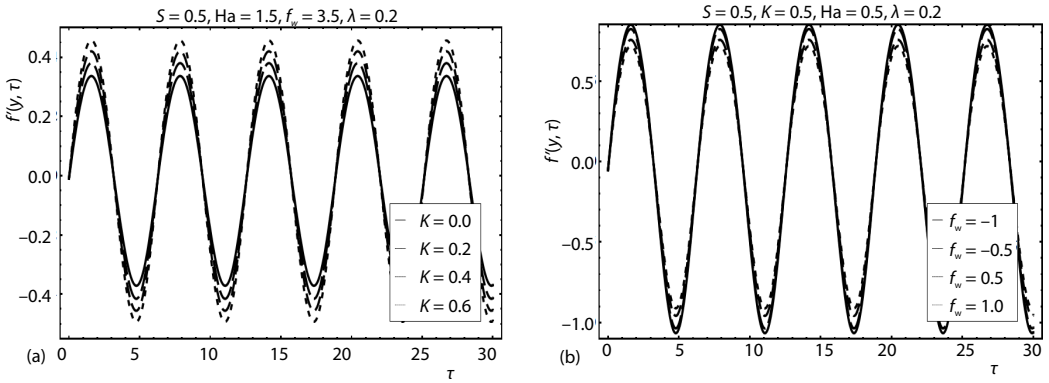

Figure 3. Velocity as function of time for various values of; (a) viscoelastic parameter *K* and (b) suction/injection parameter f_w

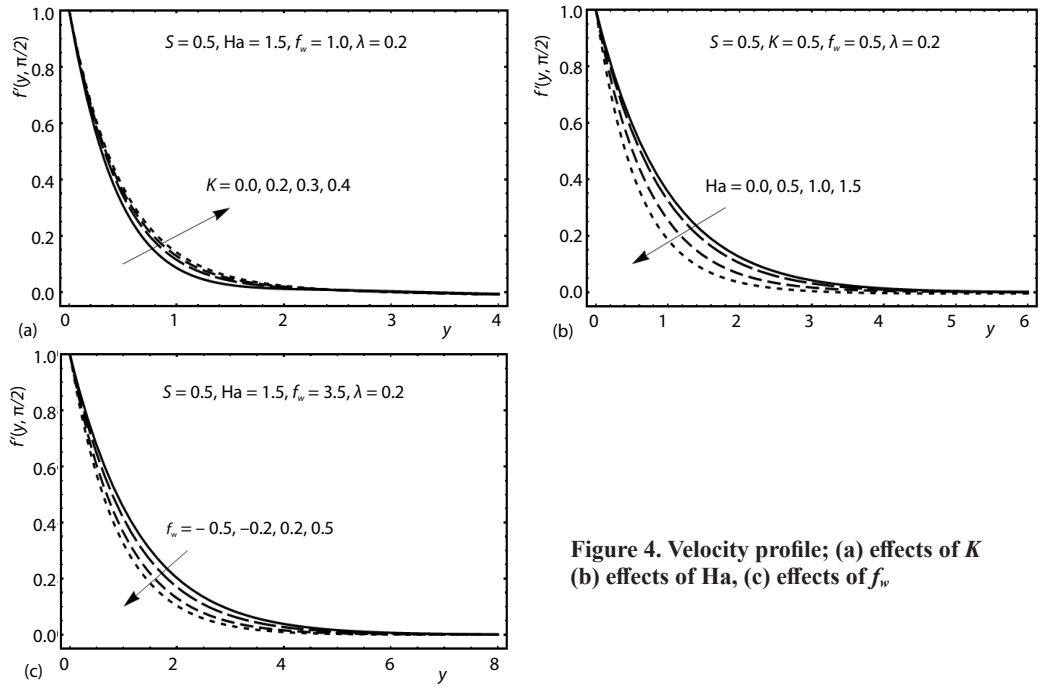

Figure 4. Velocity profile; (a) effects of K (b) effects of Ha, (c) effects of f_w

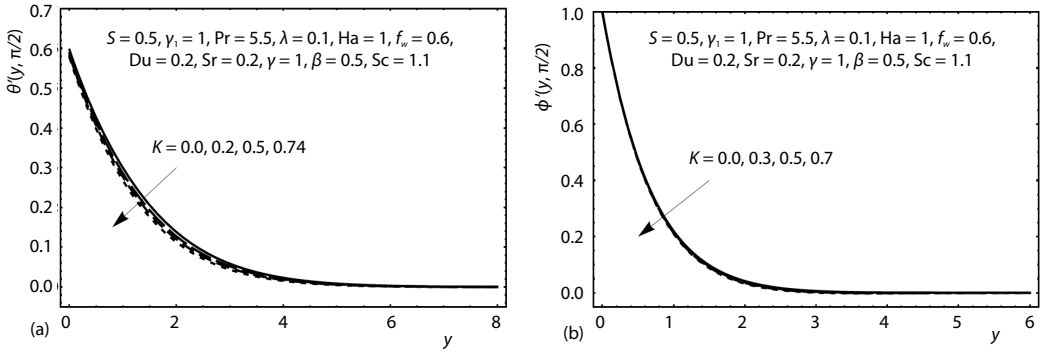

Figure 5. Effects of K on; (a) temperature and (b) concentration profiles

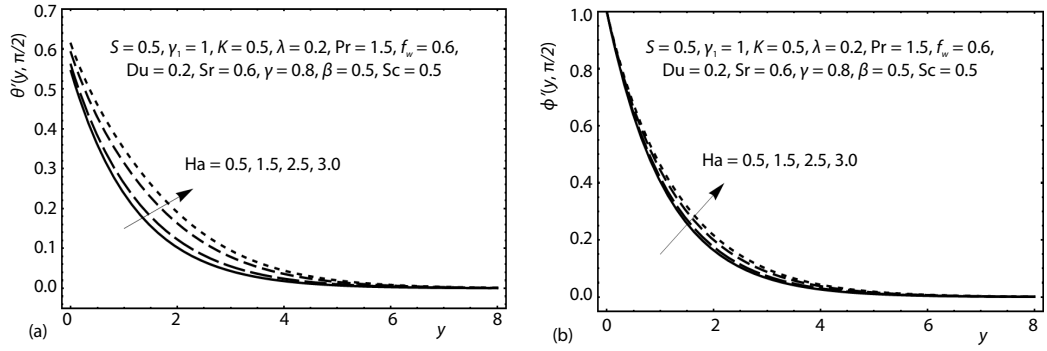

Figure 6. Effects of Hartmann number on; (a) temperature and (b) concentration profiles

Figure 6 illustrates the effects of Hartmann number on temperature and concentration profiles at $\tau = \pi/2$. The temperature inside the thermal boundary-layer is found to be enhanced with increasing Hartmann number. The variation of concentration for different values of Hartmann number is shown in fig. 6(b). It is observed that concentration profile slightly increases with increasing Hartmann number.

Figure 7 shows the variation of suction/blowing parameter on temperature and concentration profiles at $\tau = \pi/2$ by keeping other parameters constant. The dimensionless temperature inside the thermal boundary-layer is found to decrease in the case of suction. However, an increase in temperature and corresponding thermal boundary-layer thickness is noted for the injection case and corresponding thermal boundary-layer thickness increases. Similar observations are made through the examination of concentration profiles, fig. 6(b).

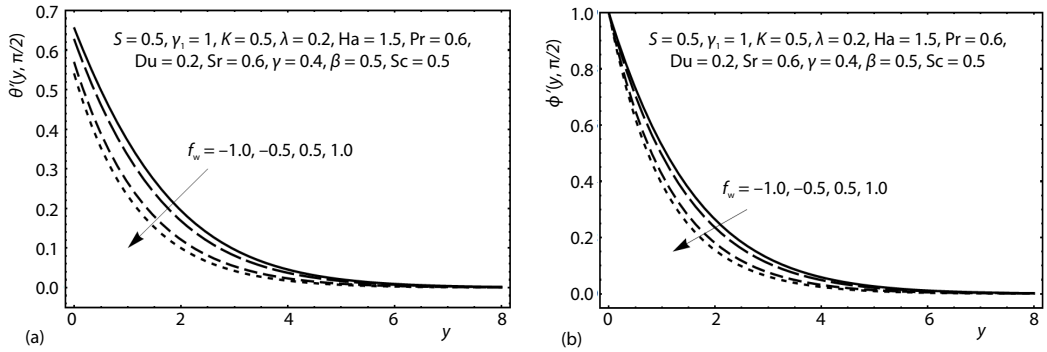

Figure 7. Effects of f_w for; (a) temperature and (b) concentration profile

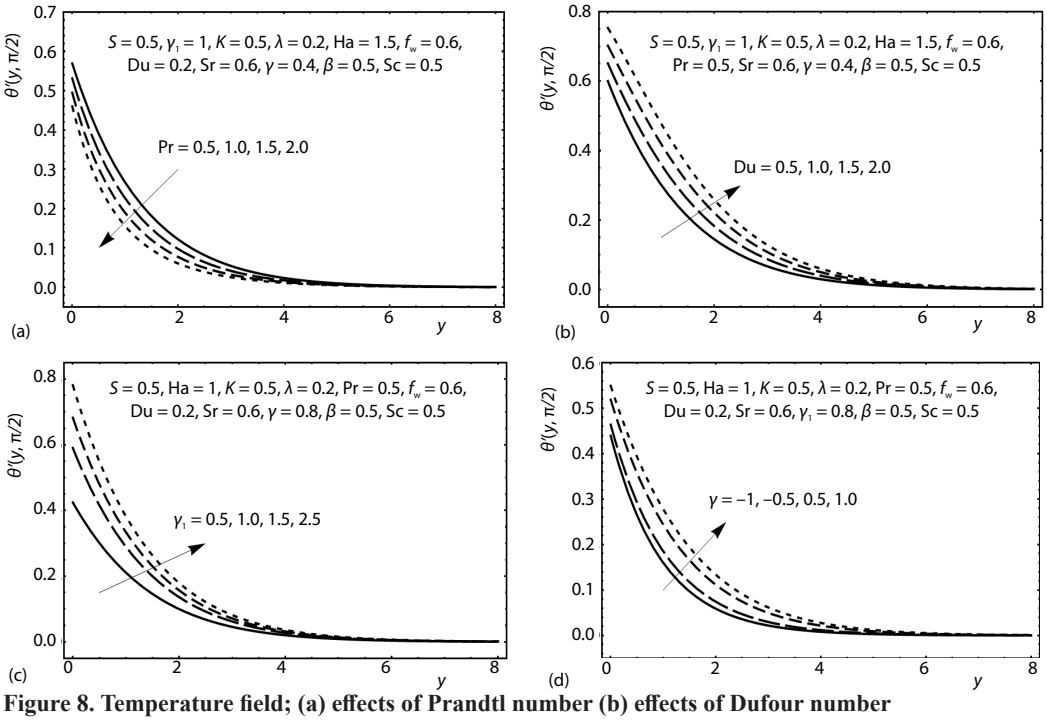

Figure 8. Temperature field; (a) effects of Prandtl number (b) effects of Dufour number (c) effects of γ_1, and (d) effects of γ

Figure 8 is sketched to see the temperature profiles for various values of Pr, Du, γ_1, and γ at $\tau = \pi / 2$. Figure 8(a) indicates that an increase of Prandtl number reduce the thickness of thermal boundary-layer. The effect of Dufour number on temperature field is shown in fig. 8(b). An increase in Dufour number leads to an increase in the temperature. The thermal boundary--layer is also found to increase for larger values of Dufour number. In fact, increase in Dufour number causes increase in energy flux due to concentration gradient which is responsible for the increases of temperature. Figure 8(c) predicts the behavior of thermal Biot number on temperature θ. With an increase in γ_1, the heat transfer coefficient increases and as a result temperature of fluid rises. Figure 8(d) depicts that temperature increases with increasing the strength of the heat generation parameter. In contrast, the temperature decreases with an increase in heat absorption parameter. This result is of key importance for the flows where heat transfer is of prime importance. The effects of Schmidt number, Soret number, and chemical reaction parameter, β,

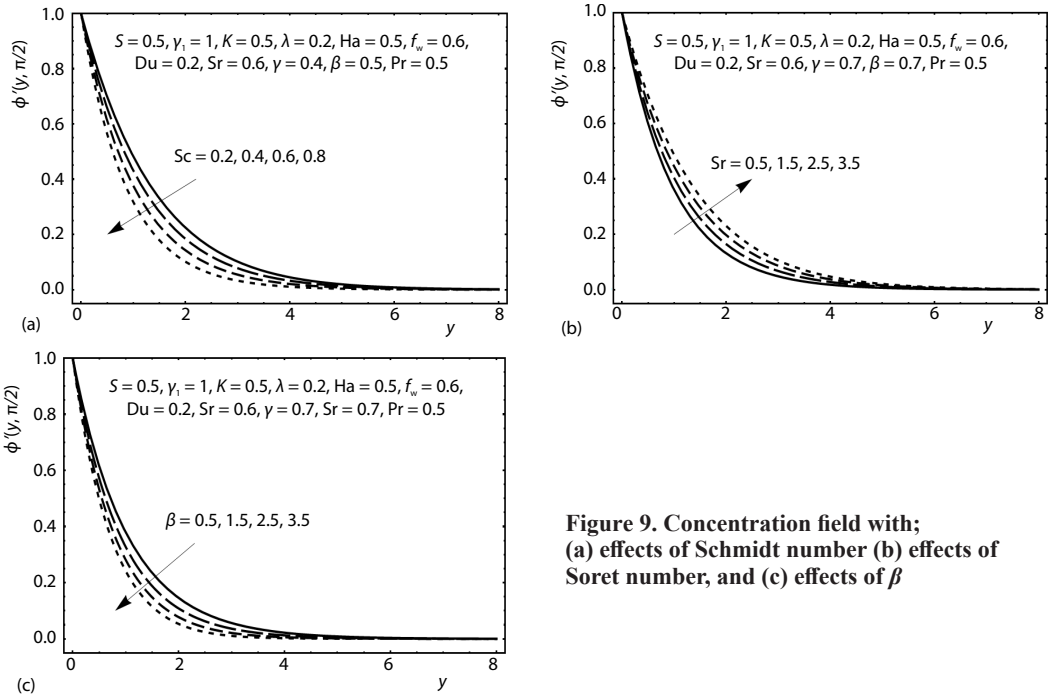

Figure 9. Concentration field with; (a) effects of Schmidt number (b) effects of Soret number, and (c) effects of β

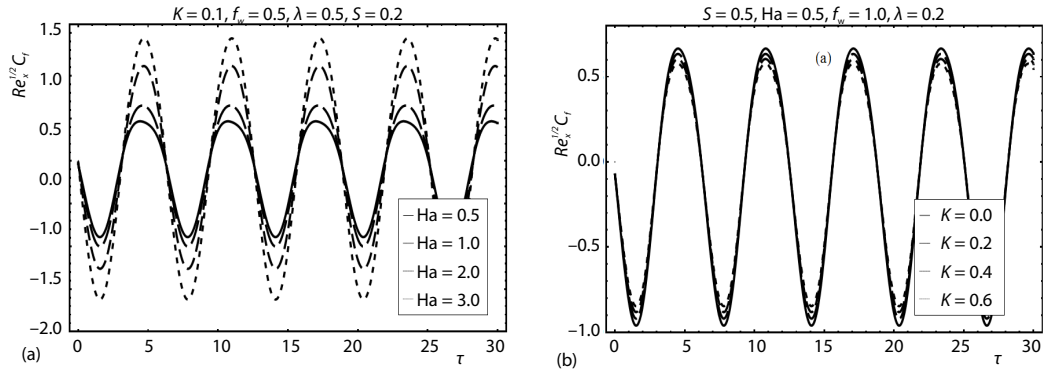

Figure 10. Time series of the skin friction $\mathrm{Re}_x^{1/2}C_f$; (a) effects of Hartmann number (b) effects of K

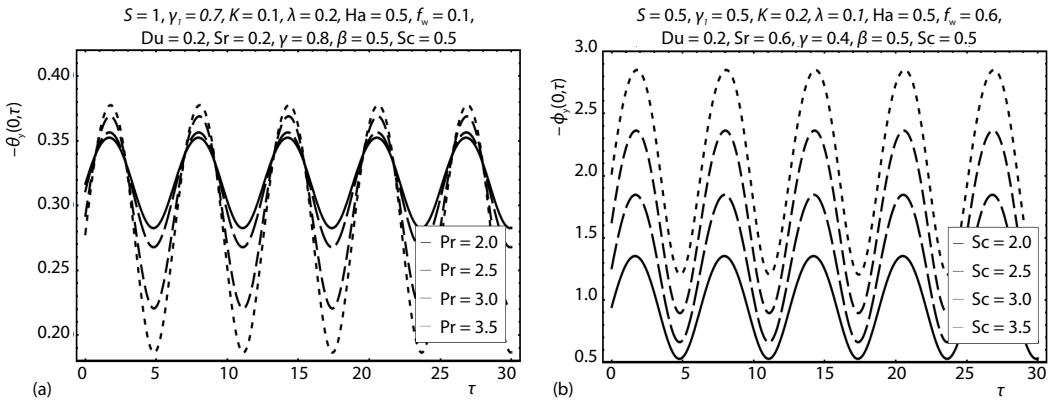

Figure 11. (a) Effects of Prandtl number on local Nusselt number $Re_x^{-1/2}Nu$ (b) effects of Schmidt number on local Sherwood number $Re_x^{-1/2}Sh$

on concentration field, ϕ, are shown in fig. 9. Figure 9(a) illustrates that as we increase Schmidt number, mass diffusion reduces and thus the concentration field decreases. Figure 9(b) depicts that increase in Soret number results in increase in concentration field. The concentration decreases with chemical reaction parameter β, fig. 9(c). Physically, larger values of β correspond to larger interfacial mass transfer rate and as a result concentration decreases.

Figure 10 illustrates the variation of wall shear stress with time for different values of Hartmann number, and Eyring-Powell fluid parameter, K. From fig. 10(a), it is observed that skin friction oscillates periodically due to the oscillatory surface and amplitude of oscillation increases with increasing Hartmann number. The effects of fluid parameter on wall shear stress are quite opposite. Here, amplitude of skin friction decreases by increasing fluid parameter. Fig-

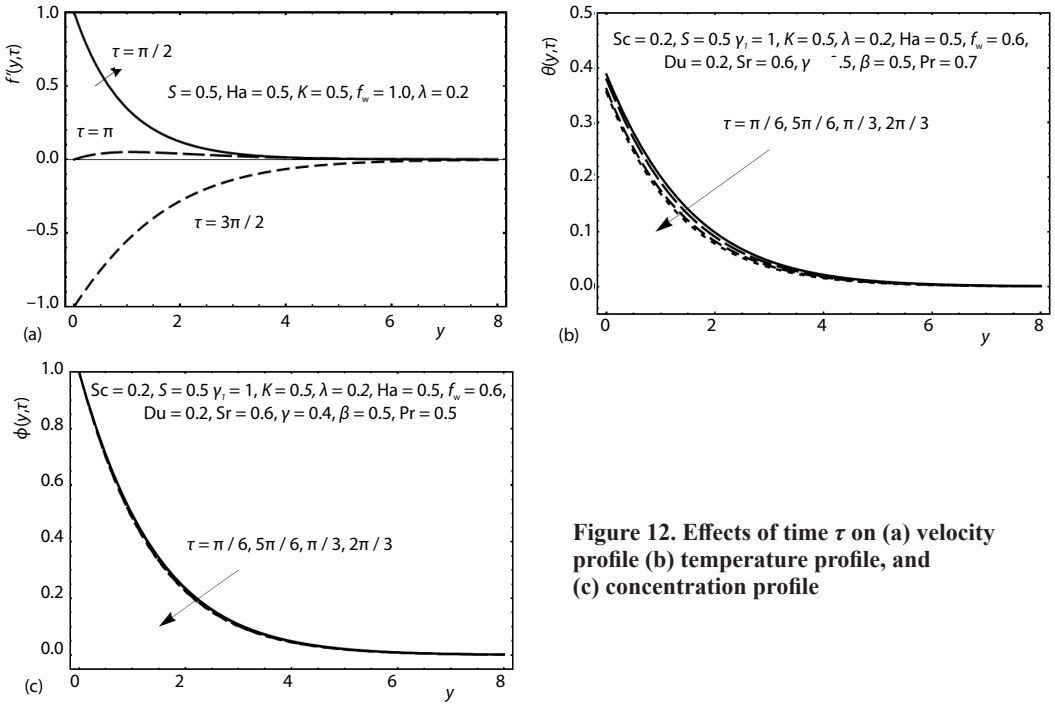

Figure 12. Effects of time τ on (a) velocity profile (b) temperature profile, and (c) concentration profile

ure 11(a) depicts the effects of Prandtl number on time-series of local Nusselt number examined by keeping other parameters constant. It is interesting to note that amplitude of local Nusselt number increases with an increase in Prandtl number. Figure 10(b) shows the on time-series of local Sherwood number for various values of Schmidt number. Here it is noted that amplitude of oscillations in local Nusselt number increases with an increase in Schmidt number.

The velocity, temperature and concentration profiles for various time instants are shown graphically in figs. 12(a)-12(c). Figure 12(a) shows that velocity component oscillates periodically between –1 to 1 because of the oscillatory nature of the sheet. Figures 12(b) and 12(c) shows that temperature and concentration profiles decrease as time increases from $\pi/6$ to $2\pi/3$.

Conclusion

This paper highlights the Soret and Dufour effects in 2-D flow of Eyring-Powell fluid over an oscillatory stretching sheet. Furthermore, heat transfer analysis is carried out in the presence of chemical reaction and convective boundary conditions. The impact of various parameters of interest is discussed graphically. The larger values of Eyring-Powell fluid parameter enhances the amplitude of velocity and boundary-layer thickness. However, opposite effects are observed in temperature and concentration profiles. Moreover, the temperature is found to decrease with increasing values of suction while it increases in the case of injection. It is also observed that the temperature and concentration field are increasing functions of Hartmann number. Similarly, temperature inside the thermal boundary-layer increases with an increase in Dufour and Biot numbers. Finally, concentration and concentration boundary-layer thickness decrease by increasing dimensionless Schmidt number and reaction rate parameter.

Acknowledgment

We are thankful to the anonymous reviewers for their useful. First author is grateful to the Higher Education Commission of Pakistan for financial assistance.

Nomenclature

c_s – concentration susceptibility
D_m – molecular diffusivity
Du – Dufour number
K, λ – non-Newtonian parameters
k – thermal conductivity of fluid
k_T – thermal diffusion ratio
k_1 – reaction rate constant
Ha – Hartmann number
Q – volumetric heat transfer
Sc – Schmidt number
Sr – Soret number
T – temperature
T_m – mean fluid temperature
v_w – suction/injection parameter
u, v – velocity component

Greek symbols

α – thermal diffusivity
β, c – Eyring-Powell model parameter
γ – heat absorption/generation parameter
γ_1 – Biot number
σ – electrical conductivity
ν – kinematic viscosity
ρ – density

References

[1] Alharbi, S. M., *et al*., Heat and Mass Transfer in MHD Viscoelastic Fluid Flow through a Porous Medium over a Stretching Sheet with Chemical Reaction, *App. Math.*, *1*, (2010), 1, pp. 446-455
[2] Hayat, T., *et al*., Heat and Mass Transfer Analysis on the Flow of a Secondgrade Fluid in Presence of Chemical Reaction, *Phys. Lett. A*, *372*, (2008), 14, pp. 2400-2408
[3] Veena, P. H., *et al*., Non-Similar Solutions for Heat and Mass Transfer Flow in an Electrically Conducting Visco-Elastic Fluid over a Stretching Sheet Embedded in a Porous Medium, *International Journal of Modern Mathematics*, *2* (2007), 1, pp. 9-26
[4] Sanjayanand, E., Khan, S. K, On Heat and Mass Transfer in a Viscoelastic Boundary Layer Flow over an Exponentially Stretching Sheet, *Int. J. Thermal Sciences, 45* (2006), 8, pp. 819-828

[5] Turkyilmazoglu, M., Multiple Solutions of Heat and Mass Transfer of MHD Slip Flow for the Viscoelastic Fluid over a Stretching Sheet, *Int. J. Thermal Sciences, 50* (2011), 11, pp. 2264-2276
[6] Hamad, M. A. A., *et al*., Radiation Effects on Heat and Mass Transfer in MHD Stagnation-Point Flow over a Permeable Flat Plate with Thermal Convective Surface Boundary Condition, Temperature Dependent Viscosity and Thermal Conductivity, *Nuclear Engineering and Design*, *242* (2012), Jan., pp. 194-200
[7] Takhar, H. S., *et al*., Flow and Mass Transfer on a Stretching Sheet with a Magnetic Field and Chemically Reactive Species, *Int. J. Eng. Sci*., *38* (2000), 12, pp. 1303-1310
[8] Afify, MHD Free Convective Flow and Mass Transfer over a Stretching Sheet with Chemical Reaction, *Heat Mass Transfer*, *40* (2004), 6-7, pp. 495-500
[9] Anghel, M., *et al*., Dufour and Soret Effects on Free Convection Boundary Layer over a Vertical Surface Embedded in a Porous Medium, Studia Universitatis Babes-Bolyai*, Mathematica, Vol. XLV* (2000), Jan, pp. 11-21
[10] Sunder, T. S., *et al*., MHD Free Convection-Radiation Interaction along a Vertical Surface Embedded in Darcian Porous Medium in Presence of Soret and Dufour's Effects, *Thermal Science, 14* (2010), 1, pp. 137-145
[11] Srinivasacharya, D., RamReddy, Ch., Soret and Dufour Effects on Mixed Convection from an Exponentially Stretching Surface, *Int. J. of Nonlinear Science*, *12* (2011), 1, pp. 60-68
[12] Beg, A., *et al*., Numerical Study of Free Convection Magnetohydrodynamic Heat and Mass Transfer from a Stretching Surface to a Saturated Porous Medium with Soret and Dufour Effects, *Comp. Materials Science*, *46* (2009), 1, pp. 57-65
[13] Cheng, C.-Y., Soret and Dufour Effects on Free Convection Boundary Layers of Non-Newtonian Power Law Fluids with Yield Stress in Porous Media over a Vertical Plate with Variable Wall heat and Mass Fluxes, *International Communications in Heat and Mass Transfer*, *38* (2011), 5, pp. 615-619
[14] Shateyi, S., *et al*., The Effects of Thermal Radiation, Hall Currents, Soret, and Dufour on MHD Flow by Mixed Convection over a Vertical Surface in Porous Media, *Mathematical Problems in Engineering, 2010*, (2010), ID 627475
[15] Zheng, L. C., *et al*., Unsteady Heat and Mass Transfer in MHD Flow over an Oscillatory Stretching Surface with Soret and Dufour effects, *Acta Mechanica Sinica*, *29* (2013), 5, pp. 667-675
[16] Ali, N., *et al*., Soret and Dufour Effects on Hydromagnetic Flow of Viscoelastic Fluid over Porous Oscillatory Stretching Sheet with Thermal Radiation, *J. Braz. Soc. Mech. Sci. Eng*., *38* (2016), 8, pp. 2533-2546
[17] Sirohi, V., *et al*., Numerical Treatment of Powell-Eyring Fluid Flow Past a 90 Degree Wedge, *Reg. J. Energy Heat Mass Transfer*, *6* (1984), 3, pp. 219-228
[18] Javed, T., *et al*., Flow of an Eyring-Powell Non-Newtonian over a Stretching Sheet, *Chemical Engineering Communications*, *200* (2012), 3, pp. 327-336
[19] Patel, M., Timol, M. G., Numerical Treatment of Powell-Eyring Fluid Flow using Method of Satisfaction of Asymptotic Boundary Conditions (MSABC), *Appl. Numer. Math*., *59* (2009), 10, pp. 2584-2592
[20] Hayat, T., *et al*., Steady Flow of an Eyring-Powell Fluid over a Moving Surface with Convective Boundary Conditions, *Int. J. Heat Mass Transfer*, *55* (2012), 7-8, pp. 1817-1822
[21] Khan, N., A., Sultana, F., On the Double Diffusive Convection Flow of Eyring-Powell Fluid Due to Cone through a Porous Medium with Soret and Dufour Effects, *Aip Advances, 5*, (2015), 5, pp. 057140
[22] Ilyas, K., *et al*., Flow of an Erying-Powell fluid over a Stretching Sheet in Presence of Chemical Reaction, *Thermal Science*, 20 (2016), 6, pp. 1903-1912
[23] Liao, S. J., The Proposed Homotopy Analysis Technique for the Solution of Non-Linear Problems, Ph. D. thesis, Shanghai Jiao Tong University, Shanghai, China, 1992
[24] Abbasbandy, S., Homotopy Analysis Method for Heat Radiation Equations, *Int. Commun. Heat Mass Transfer*, *34* (2007), 3, pp. 380-387
[25] Turkyilmazoglu, M., A Note on the Homotopy Analysis Method, *Applied Mathematics Letters*, *23* (2010), 10, pp. 1226-1230
[26] Liao, S. J., *Homotopy Analysis Method in Non-Linear Differential Equations*, Higher Education Press Beijing, Beijing, 2012

Paper submitted: August 31, 2015
Paper revised: May 21, 2016
Paper accepted: May 23, 2016